

Amphiphilic Co-networks with Moisture-Induced Surface Segregation for High-Performance Nonfouling Coatings

Yapei Wang,[†] John A. Finlay,[‡] Douglas E. Betts,[†] Timothy J. Merkel,[†] J. Christopher Luft,[†]
Maureen E. Callow,[‡] James A. Callow,[‡] and Joseph M. DeSimone^{*,†,§}

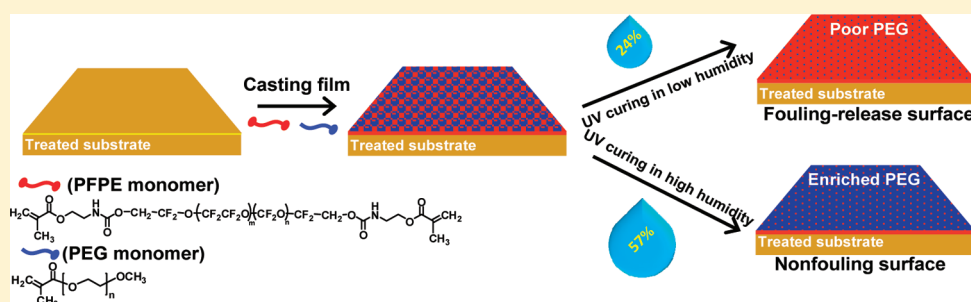
[†]Department of Chemistry, University of North Carolina at Chapel Hill, Chapel Hill, North Carolina 27599, United States

[‡]School of Biosciences, The University of Birmingham, Birmingham B15 2TT, U.K.

⁵Department of Chemical & Biomolecular Engineering, North Carolina State University, Raleigh, North Carolina 27695, United States

S Supporting Information

ABSTRACT:



Herein we report the design of a photocurable amphiphilic co-network consisting of perfluoropolyether and poly(ethylene glycol) segments that display outstanding nonfouling characteristics with respect to spores of green fouling alga *Ulva* when cured under high humidity conditions. The analysis of contact angle hysteresis revealed that the poly(ethylene glycol) density at the surface was enhanced when cured under high humidity. The nonfouling behavior of nonbiocidal surfaces against marine fouling is rare because such surfaces usually reduce the adhesion of organisms rather than inhibit colonization. We propose that the resultant surface segregation of these materials induced by high humidity may be a promising strategy for achieving nonfouling materials, and such an approach is more important than simply concentrating poly(ethylene glycol) moieties at an interface because the low surface energy has been maintained in our work.

■ INTRODUCTION

Amphiphilicity balanced by hydrophilicity and hydrophobicity has been regarded as a key element in the determination of self-assembly behavior and a critical consideration for the design and fabrication of functional materials.¹ Amphiphilic co-networks based on the intermixing of hydrophilic and hydrophobic materials belong to an emerging class of cross-linked polymeric materials with broad potential application fields ranging from biomaterials to nanotechnology.^{2–8} Recently, they have been increasingly evaluated as environmentally friendly nonfouling/fouling-release coatings^{9–15} with a utility for biofouling prevention in both marine crafts and biomedical devices.^{16–20} The combination of hydrophilic moieties within a largely hydrophobic matrix has been reported to reduce the ability of fouling entities to bind to the coating surface, enhancing the fouling resistance.^{21–23} The reason that such amphiphilic materials display nonfouling or fouling-release characteristics has been speculated as being due to nanoscale variations in the surface chemistry, topography, and mechanical properties that reduce interfacial bonding with adhesive polymers secreted by fouling organisms.^{24,25} However, from a practical point of view, a high degree of swelling of such hydrogel materials can decrease the coating robustness, enhance metal

corrosion underneath the coating, and also increase the frictional drag, limiting their practical applications in marine coatings. Reducing the contents of the hydrophilic component would resist water uptake better but at the expense of a loss of surface amphiphilicity and thus a loss in nonfouling performance. Consequently, the development of nonfouling amphiphilic coatings that exhibit low degrees of swelling in water remains a challenge.

Recently, we have developed a facile approach to fabricating amphiphilic co-networks via the photoinduced copolymerization of dimethacryloxy-functionalized hydrophobic perfluoropolyethers (PFPE-DMA) and hydrophilic monmethacryloxy-functionalized poly(ethylene glycol) (PEG-MA) segments.^{26,27} The hydrophilic adjustment of PEG, which is well known to inhibit protein as well as cell adsorption because of electrostatic repulsion and a hydration effect at the interface, could maintain water uptake within a negligible level, and the amphiphilic material displayed better fouling resistance than pure hydrophobic PFPE-DMA. During the course of these

Received: June 27, 2011

Revised: August 6, 2011

Published: August 09, 2011

studies, we recognized that the relative humidity at which we cured these amphiphilic materials gave rise to dramatically different surface properties.²⁸ In hindsight, this was not surprising because one would expect the hydrophobic, low-surface-energy perfluoropolyether segment to tend to partition to the solid/air interface at the expense of the PEG, but that would tend to be a function of the relative humidity prior to the curing reaction.^{25,29,30} To study this situation more fully, an amphiphilic PFPE/PEG co-network was photocured under exposure to various degrees of humidity, anticipating that this would lead to an enrichment in PEG character at the surface with increasing relative humidity. Herein, we show that changes in the curing environment can not only, and obviously, alter the character of the surfaces of these cross-linked amphiphilic co-networks leading to enrichment of the surfaces with PEG with increasing percent humidity but also that the fouling resistance dramatically improves as the co-networks are cured at increasing humidity. Our results suggest that at constant global chemical composition an increase in the surface segregation is what drives the outstanding nonfouling surface characteristics.

EXPERIMENTAL SECTION

Materials. Poly(ethylene glycol) monomethacrylate (PEG-MA, $M_w \approx 475$ g/mol), 2,2-diethoxyacetophenone (DEAP), and 3-(trimethoxysilyl)propyl methacrylate (TPMA) were purchased from Sigma-Aldrich and used as received. Glass slides, 1 mm \times 35 mm \times 75 mm, were purchased from Fisher and cleaned using piranha solution prior to functionalization. Perfluoropolyether-dimethacrylate, PFPE-DMA, was synthesized according to our previous work.^{26,27}

Instruments. UV–vis transparency measurements were performed on a Shimadzu UV-3600 UV–vis spectrophotometer over the wavelength range of 300–700 nm. The surface topography of the coating films was imaged using a Veeco AFM (NanoIV) in tapping mode. Static contact angles were measured using a KSV Instruments LCD CAM 200 optical contact angle meter at room temperature. All measurements were carried out with drops that had a total volume of 10 μ L on the surface of each cured film coating on glass. Dynamic tensiometry measurements were performed on a NIMA Technologies DST 9005 dynamic surface tensiometer. X-ray photoelectron spectroscopy analysis was performed by Anderson Materials Evaluation, Inc. using a Kratos Axis Ultra equipped with a monochromated Al K α X-ray source. Photoelectrons at pass energies ranging from 20 to 80 eV were collected with a concentric hemispherical analyzer and detected with a delay line detector.

RESULTS AND DISCUSSION

The cross-linked PFPE-DMA and PFPE/PEG co-networks were synthesized as previously reported.²⁷ Briefly, an optically clear blend consisting of hydrophobic difunctional PFPE-DMA and 10 wt % hydrophilic monofunctional PEG-MA was covalently cured on methacryloxy-functionalized glass substrates via UV irradiation in the presence of a photoinitiator, 2,2-diethoxyacetophenone (DEAP), under a range of humidity levels (Figure 1). It was anticipated that the PEG chains functionalized on only one chain end would be capable of reorganizing as a function of humidity even after incorporation into the cross-linked co-network. Films of these co-networks having a thickness of 0.3 mm displayed high transparency, suggesting the existence of no macroscopic phase separation in the cross-linked co-networks. The surface characteristics, surface roughness, contact angle hysteresis, and surface elemental analysis are summarized in Table 1. The surface roughness evaluated by atomic force microscopy (AFM) of the PFPE/PEG co-network cured at 57% humidity was 3 times greater than

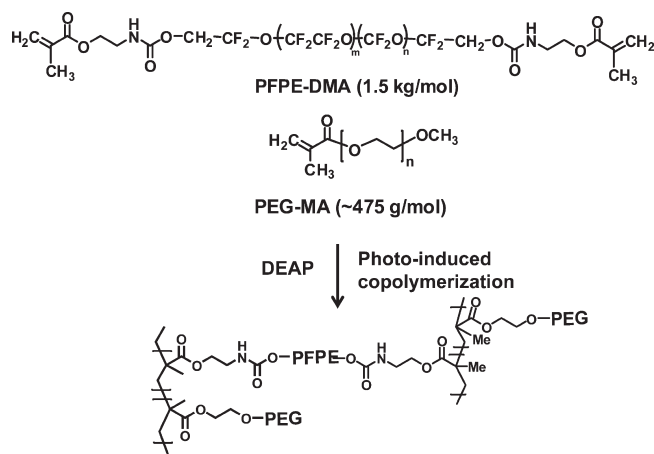


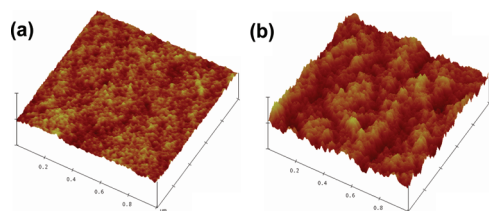
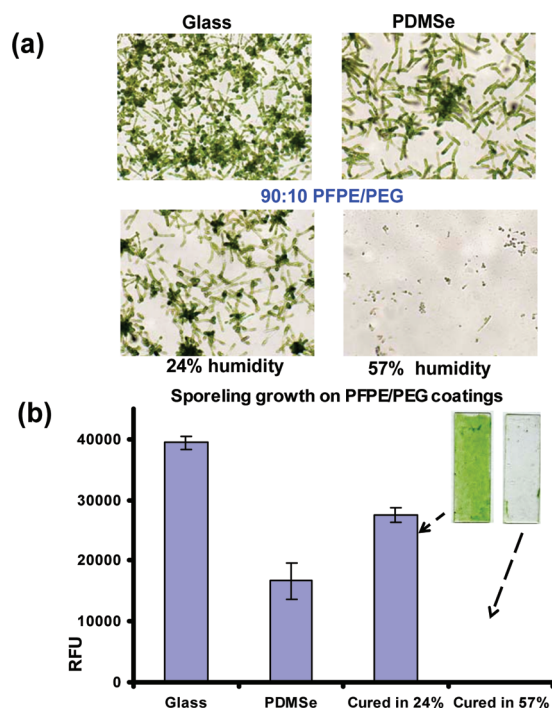
Figure 1. Synthesis route for photocured amphiphilic PFPE/PEG-MA co-networks.

that cured in 24% humidity. As shown in Figure 2, the surface topography change indicated that there was a humidity effect on the polymerized coating surface that could be induced by the enhanced phase separation between PFPE and PEG when more PEG segments were segregated at the interface. AFM analysis of the PFPE/PEG co-networks cured at 8 and 84% humidity, as shown in Figure S4, also agrees well with the surface segregation tendency upon humidity variation. X-ray photoelectron spectroscopy (XPS) analysis showed the existence of surface segregation with a higher PEG concentration found when the amphiphilic co-network was cured at higher humidity as evidenced by the lower %F and higher %C. The degree of cross-linking of the PFPE/PEG (90:10) co-network is 0.74 when regarding the degree of cross-linking as the mole fraction of monomer units that are cross-link points. As a result of the high degree of cross-linking, it was found that the hydrophobic character of the PFPE matrix prevented the coatings from appreciably swelling in water, with negligible water uptake values even after 2 weeks of immersion in 3.5% NaCl solution. Increasing PEG content could decrease the degree of cross-linking because of the lower functionality of the PEG (mono-) versus the PFPE (di-), which raised the water uptake and induced film swelling significantly.²⁷ This nonswelling behavior is critical to the long-term use of these PFPE/PEG coatings for in vivo medical device applications as well as for use in marine environments.

The biofouling characteristics of these amphiphilic materials were evaluated for application as marine coatings by exposing the materials to spores of the green fouling alga *Ulva* and then letting the settled (attached) spores germinate and develop into sporelings (young plants) using standard techniques.^{31,32} Typically, two different PFPE/PEG films with various degrees of contact angle hysteresis at a constant global chemical composition were generated by curing the materials at extensively attainable humidities of 24 and 57%. As shown in Figure 3, few spores germinated or grew into sporelings (young plants) on the PFPE/PEG coating surface cured in 57% humidity. Both standard PDMS (Silastic T2) and PFPE/PEG cured in 24% humidity showed relatively small amounts of sporelings growing on the surface in comparison to the glass standard, though this was much greater than that observed for the PFPE/PEG coating cured under high humidity. The attachment strength of the sporelings was measured by exposure to a water jet at known pressures,³² which showed that sporelings could be removed

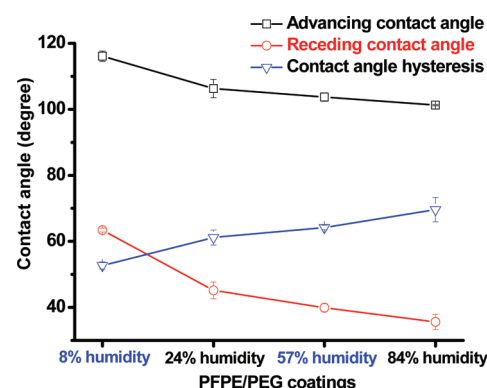
Table 1. Summarized Characterization of the 90:10 PFPE/PEG-MA Coatings Cured at Different Humidity Levels

cure humidity (%)	transparency at 550 nm (%)	water uptake (2 weeks) (%)	advancing contact angle	receding contact angle	contact angle hysteresis	surface roughness (nm)	surface analysis	
							%F	%C
24	93.9	0.52	106.3	47.4	58.9	0.52	53.03	27.90
57	94.0	0.34	103.0	38.9	64.3	1.75	50.71	30.31

**Figure 2.** AFM surface topographies of the 90:10 PFPE/PEG co-networks cured at different humidities: (a) 24 and (b) 57% humidity.**Figure 3.** Biomass of sporelings of *Ulva* on the coatings after 6 days of growth. (a) Microscope images of germinated spores that have grown into sporelings; image width 730 μm . (b) Biomass determined by a fluorescence plate reader (RFU; relative fluorescence unit). Error bars show a standard error of six replicates for each coating. The inset shows a photograph of the samples prior to exposure to the water jet.

from the 24%-humidity-coated substrate more easily than from the glass substrate (Figure S1). PFPE/PEG coatings cured in 57% humidity were classified as nonfouling because of the lack of spore attachment/development, whereas the set cured in 24% humidity was classified as fouling-release coatings, from which the fouling can be removed by the application of a water jet.

Two issues, cytotoxicity and surface segregation, were studied to understand why the same material cured at two different humidity

**Figure 4.** Dependence of the advancing contact angle, receding contact angle, and contact angle hysteresis on the environmental humidity of the photocuring polymerization. The 8 and 84% humidity levels were achieved by purging the UV chamber with dry or wet nitrogen. Humidity-level experiments at 24 and 57% humidity were performed in a humidity-controlled room in the laboratory.

levels displayed such diverse properties. Historically, nonfouling behavior has been exclusively achieved via the slow release of toxins, leading to a “non-fouling” effect.³³ With this in mind, we explored the possibility that the PFPE/PEG films cured at 57% humidity derived their nonfouling behavior from toxicity-based mechanisms. Leachates collected from coatings over 24 h after exposure to recirculating seawater for 0 or 6 days were found not to be toxic toward *Ulva* spores, thus indicating that the lack of biomass on the coating cured at 57% humidity was not due to toxicity. Additionally, as shown in Figure S2, both coating films displayed negligible cytotoxicity when incubated in a solution of HeLa cells at 37 °C for 72 h, indicating that the PFPE/PEG coatings and the collected leachate were both found to be environmentally benign (Supporting Information).

Dynamic contact angle measurements provide an implicit indication of the relative degree of interaction across the liquid/solid interface.^{34,35} The slight increase in surface roughness is an insignificant factor because of the magnitude of the roughness in determining the contact angle as the static contact angles measured for the 24 and 57% humidity coatings were observed to be 111.8 and 110.4°, respectively, which are close to their advancing contact angle results. However, for these PFPE/PEG amphiphilic coatings it was found that the receding contact angle was much lower than the advancing contact angle, presumably because of surface reconstruction when the coatings were exposed to water. This suggests that the PEG segments prefer to be in contact with the high-energy aqueous medium that drives the surface reconstruction. This hypothesis was confirmed by studying the contact angle hysteresis of 90:10 PFPE/PEG-MA coatings cured in a variety of humidity levels, as shown in Figure 4. The advancing and receding contact angles were found to decrease with increasing humidity. As such, the contact angle hysteresis gradually increased from 52° when cured in dry nitrogen (8% humidity) to 70°

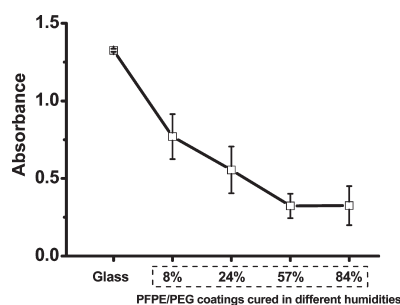


Figure 5. Amount of adsorbed fibrinogen from a 1 mg/mL solution measured by ELISA.

when cured in wet nitrogen (84% humidity). Therefore, the mobility of the PEG chains and the resulting surface reorganization from the migration of the PEG moieties to the surface are most apparent in the coating cured in high humidity.

The potential of these PFPE/PEG blends as nonfouling coating materials on medical devices was additionally determined by fibrinogen adsorption using an ELISA method.³⁶ The enzyme-induced color change in the protein solution was recorded at 450 nm as absorbance, which is proportional to the amount of antibody bound to the surfaces. To compare the amount of fibrinogen on each surface better, the absorbance on the glass substrate was set as a relative adsorption. As shown in Figure 5, all of the PFPE/PEG coatings demonstrated a certain level of resistance to fibrinogen adsorption. However, the relative adsorption was increasingly reduced as the contact angle hysteresis of PFPE/PEG was increased. Specifically, by normalizing the protein adsorption on glass as 100%, the relative protein adsorption decreased to 20% on the PFPE/PEG surfaces that were cured at high humidity above 57%. Although the quantification of fibrinogen adsorption by ELISA displays a higher value than those determined by other methods (e.g., the ¹²⁵I-radiolabeled fibrinogen method), the level on PFPE/PEG generated in high humidity is comparable to the fibrinogen adsorption on a described nonfouling surface—a densely packed, covalently bound PEG (M_w , 20 kg/mol) film on a polystyrene plate ($12 \pm 9\%$ by ELISA).³⁶

In summary, a family of photocurable PFPE/PEG amphiphilic coatings has been developed in which the surface segregation of the PEG hydrophilic segments changes on the basis of the environmental humidity at the time of curing. These transparent and robust coatings display nonfouling or fouling-release effects depending on the degree of surface segregation of the PEG moieties. It is believed that the combination of (i) low surface energy, (ii) a low degree of swelling in water, (iii) ease of processing, and (iv) low fouling properties of these materials indicates a great opportunity for this family of materials to be practically applied to prevent marine fouling for ships as well as biofouling for biomedical device coatings.

■ ASSOCIATED CONTENT

Supporting Information. Experimental details including film preparation, AFM imaging, sporeling growth, spore removal, and surface analysis by XPS. This material is available free of charge via the Internet at <http://pubs.acs.org>.

■ AUTHOR INFORMATION

Corresponding Author

*E-mail: desimone@unc.edu.

■ ACKNOWLEDGMENT

We thank the Office of Naval Research (grant no. N00014-10-10550 to J.M.D. and N00014-08-01-0010 to J.A.C./M.E.C.) for funding and the STC program of the National Science Foundation for shared facilities. Mr. Yuanchao Li is acknowledged for his help with AFM imaging.

■ REFERENCES

- (1) Wang, Y.; Xu, H.; Zhang, X. *Adv. Mater.* **2009**, *21*, 2849.
- (2) Nugay, N.; Erdodi, G.; Kennedy, J. P. *J. Polym. Sci., Part A: Polym. Chem.* **2005**, *43*, 630.
- (3) Bruns, N.; Scherble, J.; Hartmann, L.; Thomann, R.; Ivan, B.; Mulhaupt, R.; Tiller, J. C. *Macromolecules* **2005**, *38*, 2431.
- (4) Ivan, B.; Haraszti, M.; Erdodi, G.; Scherble, J.; Thomann, R.; Mulhaupt, R. *Macromol. Symp.* **2005**, *227*, 265.
- (5) Haraszti, M.; Toth, E.; Ivan, B. *Chem. Mater.* **2006**, *18*, 4952.
- (6) Tobis, J.; Thomann, Y.; Tiller, J. C. *Polymer* **2010**, *51*, 35.
- (7) Fodor, C.; Kali, G.; Ivan, B. *Macromolecules* **2011**, *44*, 4496.
- (8) Wang, Y.; Zhang, M.; Moers, C.; Chen, S.; Xu, H.; Wang, Z.; Zhang, X.; Li, Z. *Polymer* **2009**, *50*, 4821.
- (9) Gan, D.; Mueller, A.; Wooley, K. J. *Polym. Sci., Part A: Polym. Chem.* **2003**, *41*, 3531.
- (10) Gudipati, C.; Finlay, J.; Callow, J.; Callow, M.; Wooley, K. *Langmuir* **2005**, *21*, 3044.
- (11) Krishnan, S.; Ayothi, R.; Hexmer, A.; Finlay, J.; Sohn, K.; Perry, R.; Ober, C.; Krammer, E.; Callow, M.; Callow, J.; Fisher, D. *Langmuir* **2006**, *22*, 5075.
- (12) Martinelli, E.; Agostini, S.; Galli, G.; Chiellini, E.; Glisenti, A.; Pettitt, M. E.; Callow, M. E.; Callow, J. A.; Graf, K.; Bartels, F. W. *Langmuir* **2008**, *24*, 13138.
- (13) Finlay, J.; Krishnan, S.; Callow, M.; Callow, J.; Dong, R.; Asgill, N.; Wong, K.; Kramer, E.; Ober, C. *Langmuir* **2008**, *24*, 503.
- (14) Martinelli, E.; Suffredini, M.; Galli, G.; Glisenti, A.; Pettitt, M. E.; Callow, M. E.; Callow, J. A.; Williams, D.; Lyall, G. *Biofouling* **2011**, *27*, 529.
- (15) Sundaram, H. S.; Cho, Y.; Dimitriou, M. D.; Weinmann, C. J.; Finlay, J. A.; Cone, G.; Callow, M. E.; Callow, J. A.; Kramer, E. J.; Ober, C. K. *Biofouling* **2011**, *27*, 589.
- (16) Omae, I. *Chem. Rev.* **2003**, *103*, 3431.
- (17) Chen, S.; Zheng, J.; Li, L.; Jiang, S. *J. Am. Chem. Soc.* **2005**, *127*, 14473.
- (18) Swain, G. *Prot. Coat. Eur.* **1999**, *4*, 18.
- (19) Grunlan, M.; Lee, N.; Cai, G.; Gädda, T.; Mabry, J.; Mansfeld, F.; Kus, E.; Wendt, D.; Kowalke, G.; Finlay, J.; Callow, J.; Callow, E.; Weber, W. *Chem. Mater.* **2004**, *16*, 2433.
- (20) Schumacher, J.; Long, C.; Callow, M.; Finlay, J.; Callow, J.; Brennan, A. *Langmuir* **2008**, *24*, 4931.
- (21) Langer, R. *Nature* **1998**, *392*, 5.
- (22) Chapman, R.; Ostuni, E.; Takayama, S.; Holmlin, R.; Yan, L.; Whitesides, G. J. *Am. Chem. Soc.* **2000**, *122*, 8303.
- (23) Herrwerth, S.; Eck, W.; Reinhardt, S.; Grunze, M. *J. Am. Chem. Soc.* **2003**, *125*, 9359.
- (24) Rana, D.; Matsuura, T. *Chem. Rev.* **2010**, *110*, 2448.
- (25) Weinman, C. J.; Gunari, N.; Krishnan, S.; Dong, R.; Paik, M. Y.; Sohn, K. E.; Walker, G. C.; Kramer, E. J.; Fischer, D. A.; Ober, C. K. *Soft Matter* **2010**, *6*, 3237.
- (26) Hu, Z.; Chen, L.; Betts, D. E.; Pandya, A.; Hillmyer, M. A.; DeSimone, J. M. *J. Am. Chem. Soc.* **2008**, *130*, 14244.
- (27) Wang, Y.; Betts, D.; Finlay, J.; Brewer, L.; Callow, M.; Callow, J.; Wendt, D.; DeSimone, J. *Macromolecules* **2011**, *44*, 878.
- (28) Yarbrough, J.; Rolland, J.; DeSimone, J.; Callow, M.; Finlay, J.; Callow, J. *Macromolecules* **2006**, *39*, 2521.
- (29) Crowe-Willoughby, J.; Genzer, J. *Adv. Funct. Mater.* **2009**, *19*, 460.
- (30) Walton, D.; Soo, P.; Mayes, A.; Sofia Allgor, S.; Fujii, J.; Griffith, L.; Ankner, J.; Kaiser, H.; Johansson, J.; Smith, G.; Barker, J.; Satija, S. *Macromolecules* **1997**, *30*, 6947.

- (31) Weinman, C. J.; Finlay, J. A.; Park, D.; Paik, M. Y.; Krishnan, S.; Sundaram, H.; Dimitriou, M.; Sohn, K. E.; Callow, M. E.; Callow, J. A.; Handlin, D. L.; Willis, C. L.; Kramer, E. J.; Ober, C. K. *Langmuir* **2009**, *25*, 12266.
- (32) Finlay, J. A.; Fletcher, B. R.; Callow, M. E.; Callow, J. A. *Biofouling* **2008**, *24*, 219.
- (33) Thomas, K. V.; Brooks, S. *Biofouling* **2010**, *26*, 73.
- (34) Markal, U.; Uslu, N.; Wynne, K. J. *Langmuir* **2007**, *23*, 209.
- (35) Makal, U.; Wynne, K. J. *Langmuir* **2005**, *21*, 3742.
- (36) Zhang, Z.; Chao, T.; Shen, S.; Jiang, S. *Langmuir* **2006**, *22*, 10072.